

Blind Compressed Sensing Dynamic MRI

Sajan Goud Lingala¹ and Mathews Jacob²

¹Biomedical Engineering, The University of Iowa, Iowa city, IA, United States, ²Electrical and Computer Engineering, The University of Iowa, IA, United States

Introduction: Achieving high spatio-temporal resolutions in dynamic MRI (DMRI) (eg. myocardial perfusion MRI) is often challenging due to the slow nature of MR acquisitions. Recently, several schemes that exploit the low-rank property of dynamic datasets were introduced to accelerate dynamic MRI [eg: 1-3]. These methods exploit the similarity of the voxel time profiles (intensity variations as a function of time) by expressing them as a linear combination of a few orthogonal temporal basis functions. Since the temporal bases and their coefficients (spatial weights) are estimated from the under-sampled Fourier data itself, this representation is termed as the blind linear model (BLM). This method provides good image quality at high accelerations, when the inter-frame motion is not very significant. However, the similarity of voxel profiles often degrades significantly with inter-frame motion (eg. free breathing perfusion). Since more basis functions, and equivalently more coefficients, are required to accurately represent the resulting dataset using BLM, the maximum acceleration that can be achieved using BLM degrades significantly with inter-frame motion.

To overcome this, we introduce a novel dynamic imaging algorithm, based on blind compressed sensing (BCS) [4]. We model the time profiles of each voxel as a *sparse* linear combination of temporal basis functions from a *large dictionary* (see Fig 1). Similar to BLM, the temporal basis functions and spatial weights are estimated from the under-sampled Fourier data. Note that the representation is locally low-rank since the time-profiles are expressed as the linear combination of very few basis functions. Since very few coefficients of this representation are non-zero at each voxel, the number of unknowns or degrees of freedom (DOF) of this representation is much smaller than that of BLM. Specifically, the huge saving in the number of non-zero coefficients dwarf the slight increase in DOF due to the higher number of temporal basis functions (since the number of voxels are much larger than the number of time frames). Hence, we expect this scheme to provide improved image quality at high accelerations, even when the dataset is corrupted with high inter-frame motion.

Methods: We model the Casorati matrix of the DMRI dataset as the product of a sparse coefficient matrix $\mathbf{U}_{m \times R}$ and a dictionary of temporal basis functions, specified by $\mathbf{V}_{R \times n}$ (see Fig. 1). Here m, n and R are the numbers of voxels in each frame, total time frames, and the number of temporal basis functions, respectively. Specifically, we pose the simultaneous estimation of the matrices \mathbf{U} and \mathbf{V} , subject to data-consistency constraints, as:

$$\{\mathbf{U}^*, \mathbf{V}^*\} = \arg \min_{\mathbf{U}, \mathbf{V}} \|\mathbf{A}(\mathbf{U}\mathbf{V}) - \mathbf{b}\|_2^2 + \lambda_1 \|\mathbf{U}\|_{l_1} + \lambda_2 \|\mathbf{V}\|_F^2 \quad (1)$$

Here \mathbf{A} is the Fourier sampling operator that acquires the measurements \mathbf{b} on a specified k - t trajectory. We consider a sparsity promoting l_1 norm on \mathbf{U} and an energy preserving Frobenius norm on \mathbf{V} . These regularizations ensure that the above problem is well-posed. We use a majorize-minimize strategy to decompose (1) into simpler sub problems. Specifically, we approximate the l_1 penalty with a Huber penalty, parameterized by a single parameter β [see 5 for details]:

$$\{\mathbf{U}^*, \mathbf{V}^*\} = \arg \min_{\mathbf{U}, \mathbf{V}, \mathbf{L}} \|\mathbf{A}(\mathbf{U}\mathbf{V}) - \mathbf{b}\|_2^2 + \lambda_1 \|\mathbf{L}\|_{l_1} + \lambda_2 \|\mathbf{V}\|_F^2 \quad s.t., \mathbf{U} = \mathbf{L} \quad (2)$$

$$\{\mathbf{U}^*, \mathbf{V}^*\} = \arg \min_{\mathbf{U}, \mathbf{V}, \mathbf{L}} \|\mathbf{A}(\mathbf{U}\mathbf{V}) - \mathbf{b}\|_2^2 + \lambda_1 \|\mathbf{L}\|_{l_1} + \frac{\beta}{2} \|\mathbf{U} - \mathbf{L}\|_F^2 + \lambda_2 \|\mathbf{V}\|_F^2 \quad (3)$$

For a fixed β , the algorithm iterates between three simple steps of (a) shrinkage of \mathbf{L} , (b) solving a quadratic problem in \mathbf{U} and (c) solving a quadratic problem in \mathbf{V} . We use fast conjugate gradient (CG) solvers to solve (b) and (c). We start with a small value of β and gradually increase it within the loop. The Huber approximation of the l_1 norm is essentially the Frobenius norm, when β is small. According to [6], the solution of the resulting problem is the nuclear norm solution when $R \gg \text{rank of the signal matrix}$. Thus, we start with the nuclear norm solution and gradually enforce the sparsity of the coefficients/spatial weights. This approach makes the algorithm less sensitive to local minima issues.

Example: In Fig. 2, we compare the BCS scheme with the BLM model, which uses nuclear norm minimization [3]. We retrospectively under-sample a myocardial perfusion data set (190x90x70), acquired using FLASH sequence on a Siemens 3T scanner (TR/TE=2.5/1.5ms). There is significant motion due to improper gating and breathing (see temporal profiles in Fig. 2.b). We sample each of the images using 12 uniformly spaced radial lines in k -space. The lines were randomly rotated for different frames. This pattern corresponds to an acceleration of 7.5, compared to Cartesian sampling. We consider $R=45$ basis functions in the dictionary. The reconstructions show that the BCS scheme is able to recover the subtle spatial features with minimal temporal blurring. In contrast, we observe heavy temporal blurring in the BLM reconstructions, resulting in loss of details such as the borders of the heart and the papillary muscles. We observe similar trends, when we compare BCS with other low rank schemes such as the greedy incremented rank power factorization [2] and the minimum non-convex Schatten p -norm scheme; these results are not reported here due to lack of space.

Discussion: We proposed a novel scheme based on blind compressed sensing in dynamic MRI. Our experiments demonstrate that this model provides reduced blurring and artifacts over low-rank methods, when dynamic datasets with significant inter-frame motion is considered.

Acknowledgement: NSF Awards CCF-0844812, CCF-1116067 for the funding and Dr. Edward DiBella, University of Utah for the data used in fig 2.

References: [1] Z.Liang et al, ISBI 2007 [2] J.Haldar et al, ISBI 2010 [3] S.Goud Lingala et al, IEEE-TMI 2011 [4] S Gleichman IEEE-Trans Inf Theory 2010 [5] Y.Hu et al, IEEE-TIP 2011 [6] B.Recht et al, SIAM Review 2010.

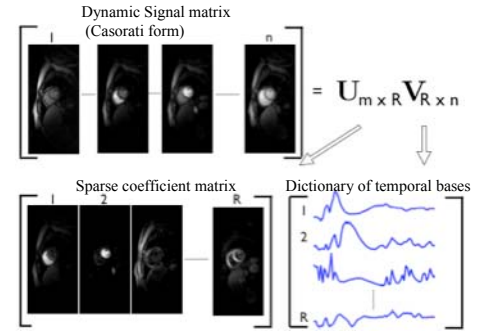


Fig1: Blind compressed sensing (BCS) model: The temporal profile of each voxel of the dataset is modeled as a sparse weighted linear combination of temporal bases, picked from a dictionary \mathbf{V} . The sparse coefficients/weights of the basis functions correspond to the columns of \mathbf{U} , while the basis functions correspond to the rows of \mathbf{V} . Note that the 1st and 2nd columns of \mathbf{U} correspond to right and left ventricles, while the 1st and 2nd rows of \mathbf{V} are the temporal profiles of these regions.

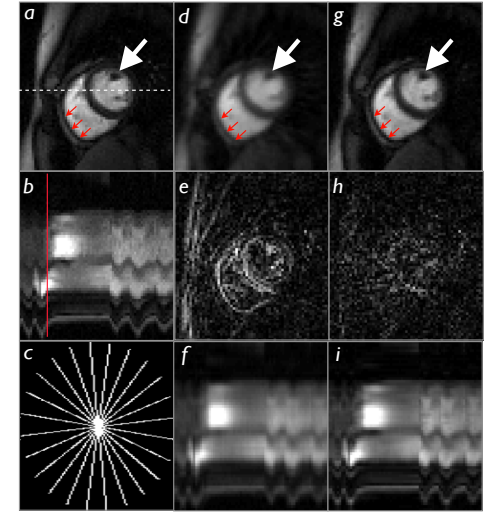


Fig 2: Reconstruction from 7.5 fold under-sampled data. (a) One time frame of the fully sampled dataset, corresponding to a frame with large motion. (b) The time profile (through the dotted line in (a)), which depicts the perfusion dynamics and respiratory motion. (c) Sampling pattern for one frame (d-f) A frame of the BLM reconstruction, its temporal profile, and the error (g-i) blind compressed sensing (BCS) reconstruction. Note that BCS preserves the fine details compared to BLM scheme, especially at the white arrows. Also see the resolution of papillary muscles and the red arrows. The differences are depicted in the error images as well. A similar trend is observed in other frames.